nature nanotechnology

Article

https://doi.org/10.1038/s41565-023-01478-0

# A free-standing lithium phosphorus oxynitride thin film electrolyte promotes uniformly dense lithium metal deposition with no external pressure

In the format provided by the authors and unedited

# Table of contents

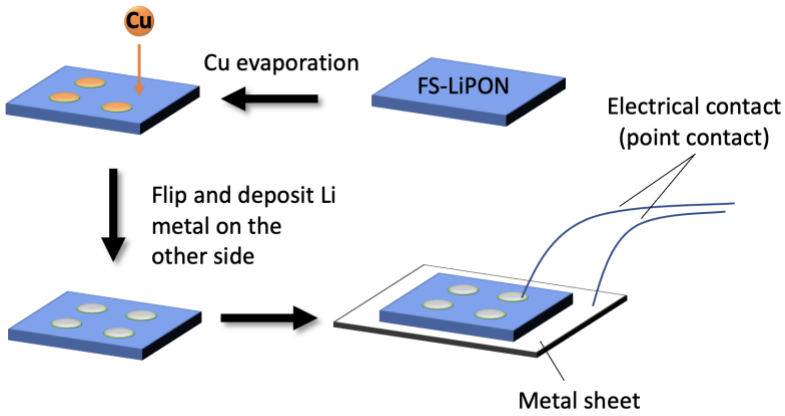


**Supplementary Fig. 1 Schematic of testing configuration for Li-Cu FS-LiPON cell cycling**.

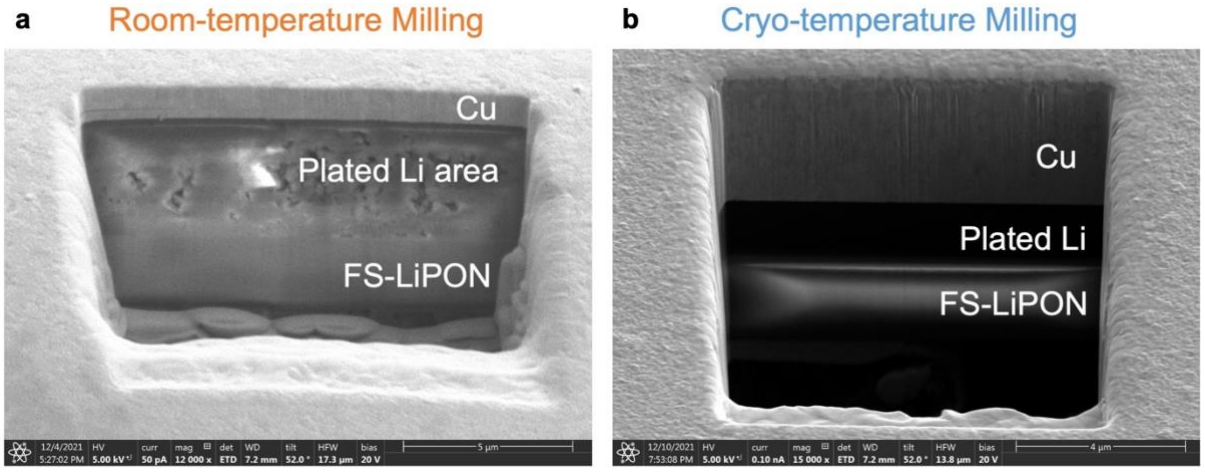


**Supplementary Fig. 2 Comparison of cross sections from Li metal sample milled at room temperature and cryogenic temperature (-185 °C).** Cross-section FIB/SEM of the Li-Cu cell with ion milling performed at room temperature (**a**) and cryogenic temperature (**b**). Morphology and contrast of plated Li metal in (**a**) have been changed due to the lack of cryogenic protection compared with (**b**).

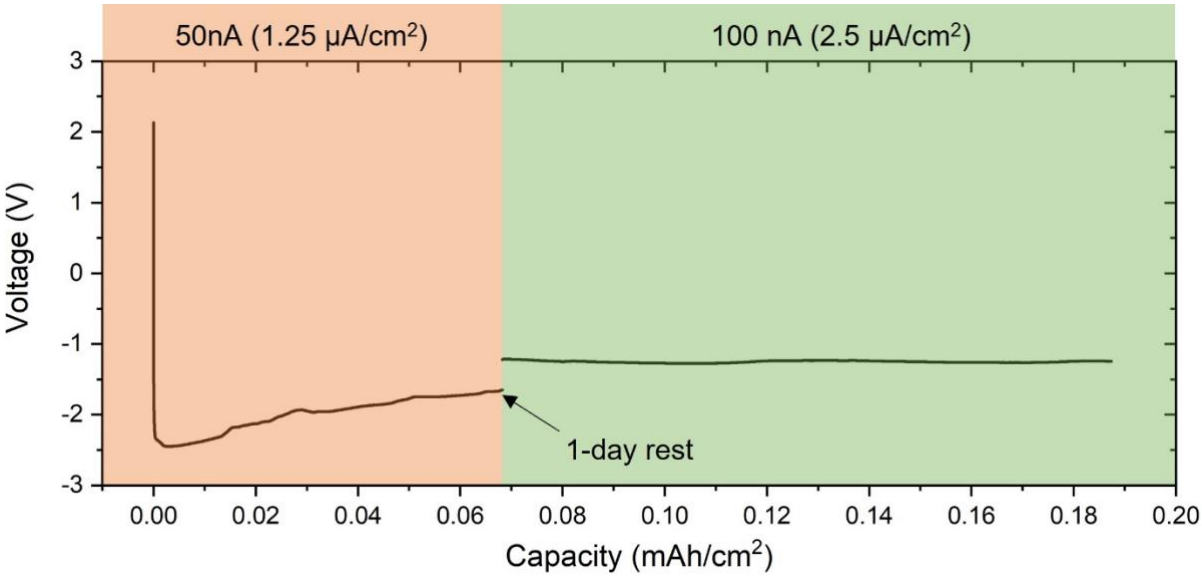


**Supplementary Fig. 3 Voltage curve of Li metal plating with 1-day rest step.**

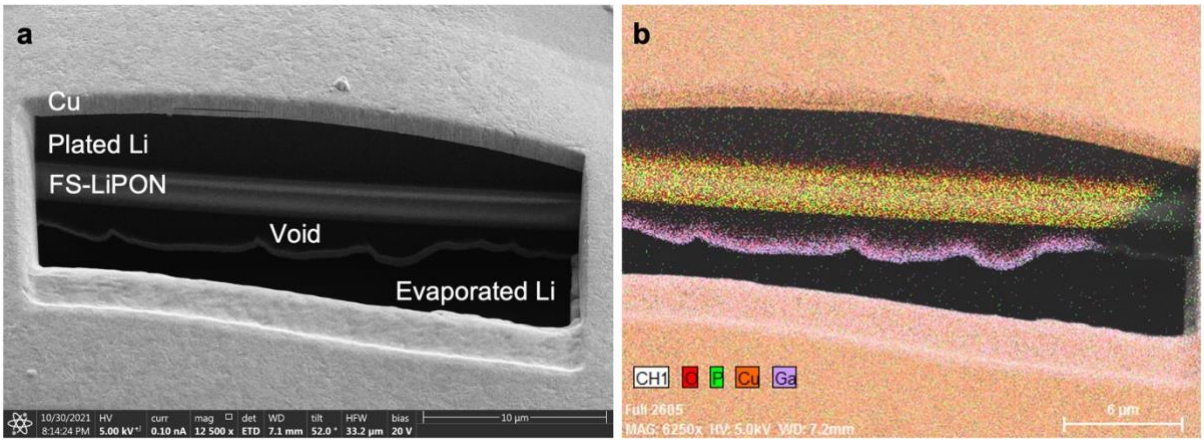


**Supplementary Fig. 4 Li metal morphology after plating. a**, Cross-section cryo-FIB/SEM image of the Li-Cu cell after plating. **b**, EDS mapping of the corresponding area in (**a**).

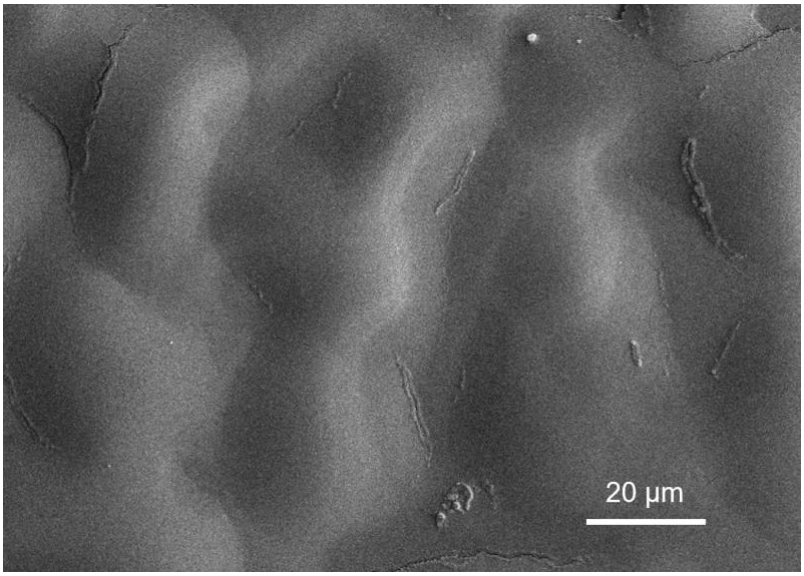


**Supplementary Fig. 5 Top-view SEM image of Cu surface on the Li-Cu cell after Li metal plating.**

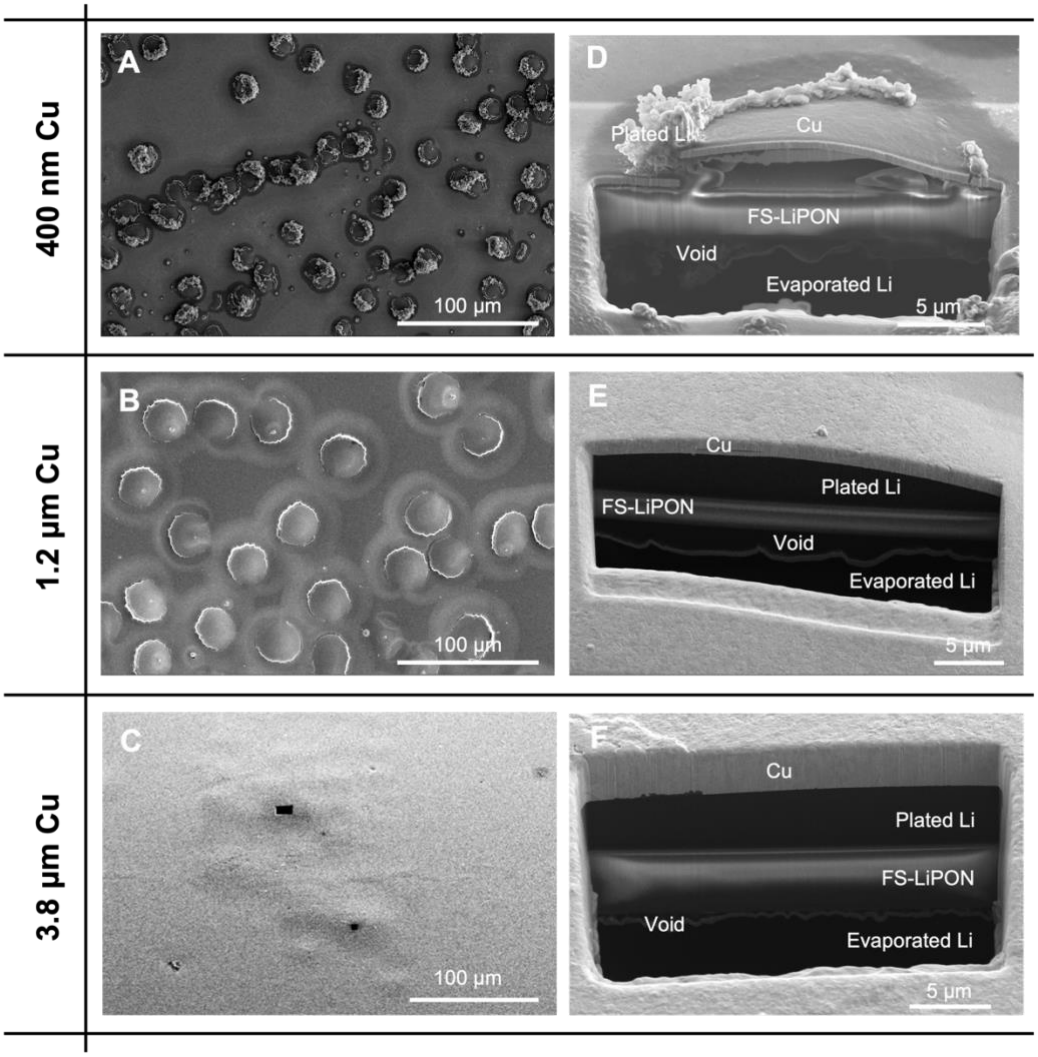


**Supplementary Fig. 6 Top-view and cross-section SEM images of Li-Cu cell with different Cu thicknesses.**

**a**

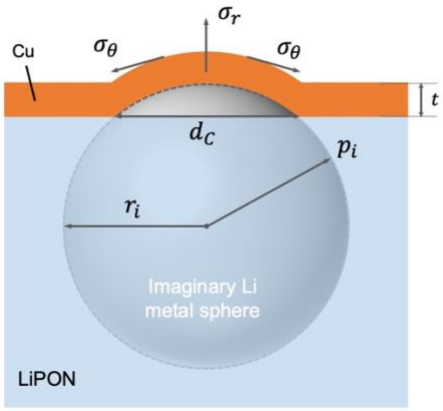


$$P_i = \frac{\varepsilon_{Cu} E_{Cu}}{(1-\nu_{Cu})} \cdot \left\{ \frac{3(r_i+t)^3}{2\left[(r_i+t)^3 - r_i^3\right]} - \frac{\nu_{Cu}}{1-\nu_{Cu}} \right\}^{-1} \quad (1)$$

$\varepsilon_{Cu}$: Strain in the circumferential directions
$E_{Cu}$ :Young's modulus of Cu CC
$t$: Thickness of Cu CC
$d_C$: Chord length inside Li sphere under Cu
$r_i$: Radius of Cu CC imaginary sphere
$\kappa$: Curvature of Cu CC
$\nu_{Cu}$: Poisson's ratio of Cu

**b**

| | **400 nm Cu** | **1.2 μm Cu** | **3.8 μm Cu** |
|---|---|---|---|
| $\varepsilon_{Cu}$ | 0.052 | 0.030 | 0.024 |
| $E_{Cu}$ / GPa | 130 | 130 | 130 |
| $t$ / μm | 0.4 | 1.2 | 3.8 |
| $r_i$ / μm | 16.036 | 54.054 | 227.273 |
| $\nu_{Cu}$ | 0.34 | 0.34 | 0.34 |
| $P_i$ (= $\sigma_r$) / GPa | **0.503** | **0.260** | **0.151** |

**Supplementary Fig. 7 Stress analysis on Li-Cu cell with different Cu thicknesses. a,** Schematic of the model used for interfacial stress estimation and corresponding formula (1). **b**, parameters and calculated stresses at Li/Cu interface with different Cu thicknesses. The radii of the imaginary spheres were converted from Li metal sphere curvatures, which were measured by ImageJ software using the cross-section images shown in **Supplementary Fig. 6 d-f.**

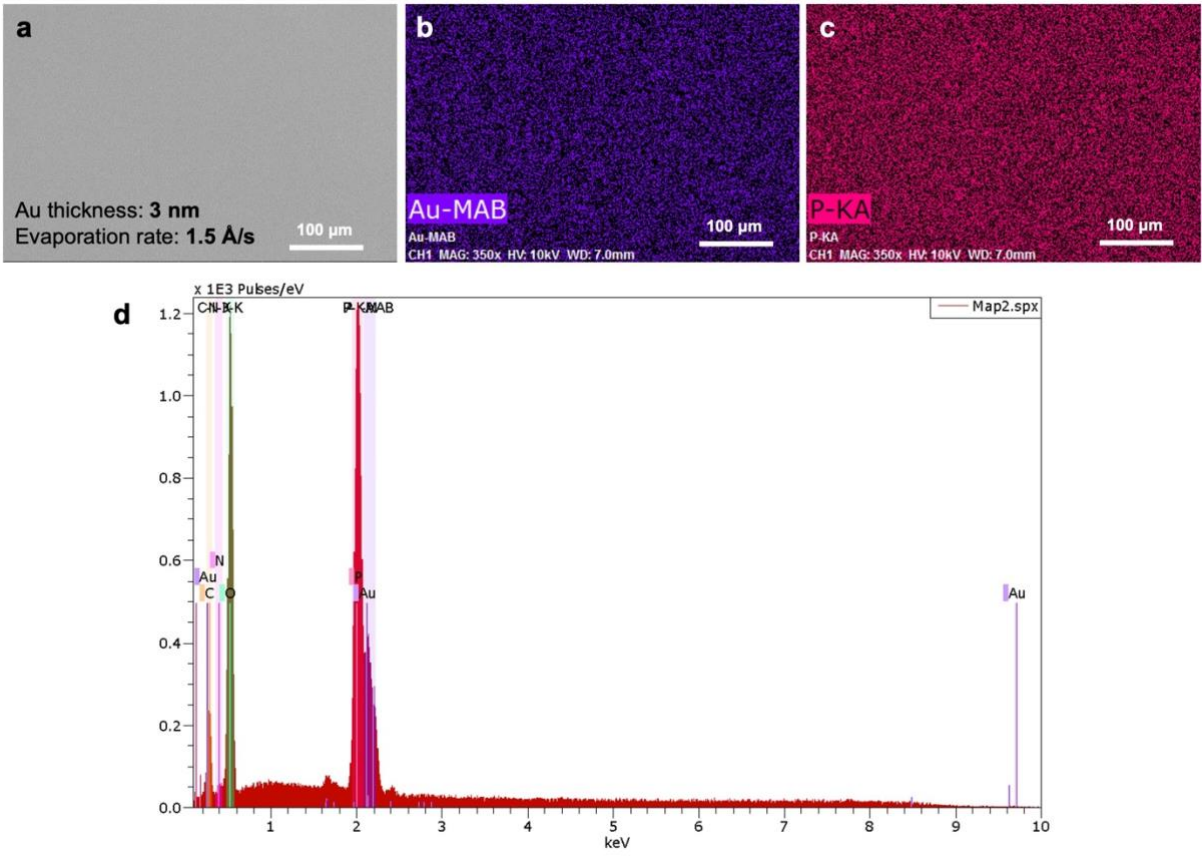


**Supplementary Fig. 8 Au deposition on FS-LiPON as a seeding layer. a**, Top-view SEM image of Au seeding layer on FS-LiPON. Au film thickness is 3 nm. **b, c**, EDS mapping results of Au signal (**b**) and P signal (**c**) in the same region, demonstrating the uniform evaporation of Au on FS-LIPON. **d**, EDS spectrum collected from the region shown in (**a**).

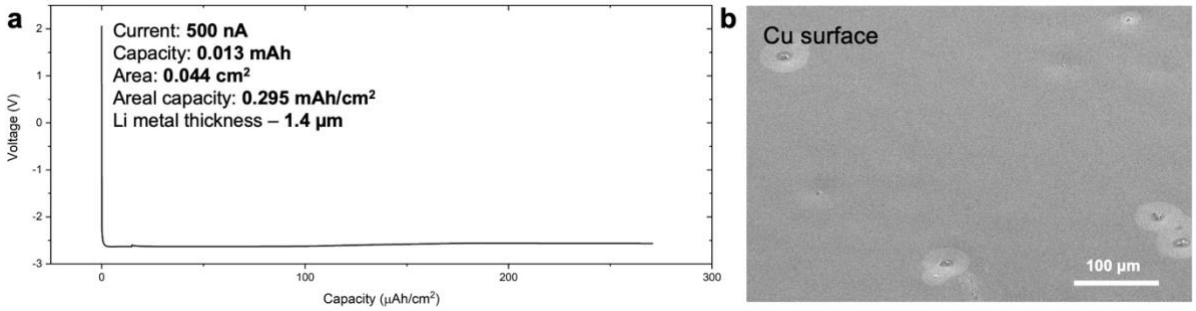


**Supplementary Fig. 9 FS-LiPON Li-Cu cell plated with Au seeding layer. a**, Voltage curve of Li metal plating in Li-Cu cell with Au seeding layer. **b**, Surface morphology of plated Li-Cu cell, showing a relatively smooth Cu surface and indicating uniform Li metal deposition.

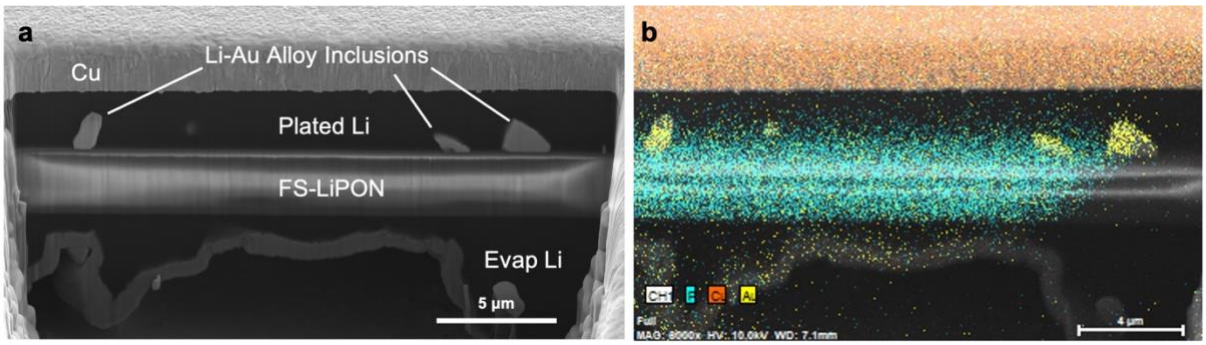


**Supplementary Fig. 10 SEM observation of Li-Au alloy inclusion in plated Li metal. a**, Cross-section image of plated Li-Cu cell with Au seeding layer. Plated Li metal in this cell is ~3 µm in thickness. Inclusions within plated Li layer can be seen. **b**, EDS mapping at the region shown in (**a**), suggesting the inclusions are Au-containing species.

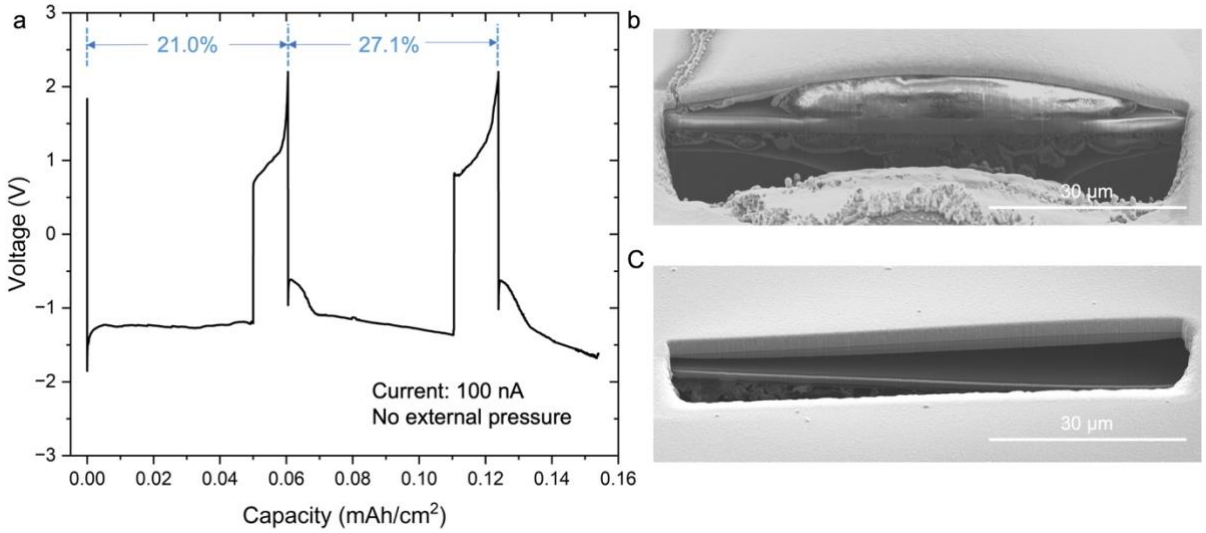


**Supplementary Fig. 11 FS-LiPON Li-Cu cell cycling without external pressure. a**, Voltage curve of Li-Cu FS-LiPON cell cycled with a current of 100 nA under no external pressure. **b**, Cross-section image of Li-Cu cell with Au seeding layer after cycling. Li metal layer appears charging under SEM. **c**, Cross-section image of Li-Cu cell with Au seeding layer after cycling with a gap formed between Cu and FS-LiPON layers.

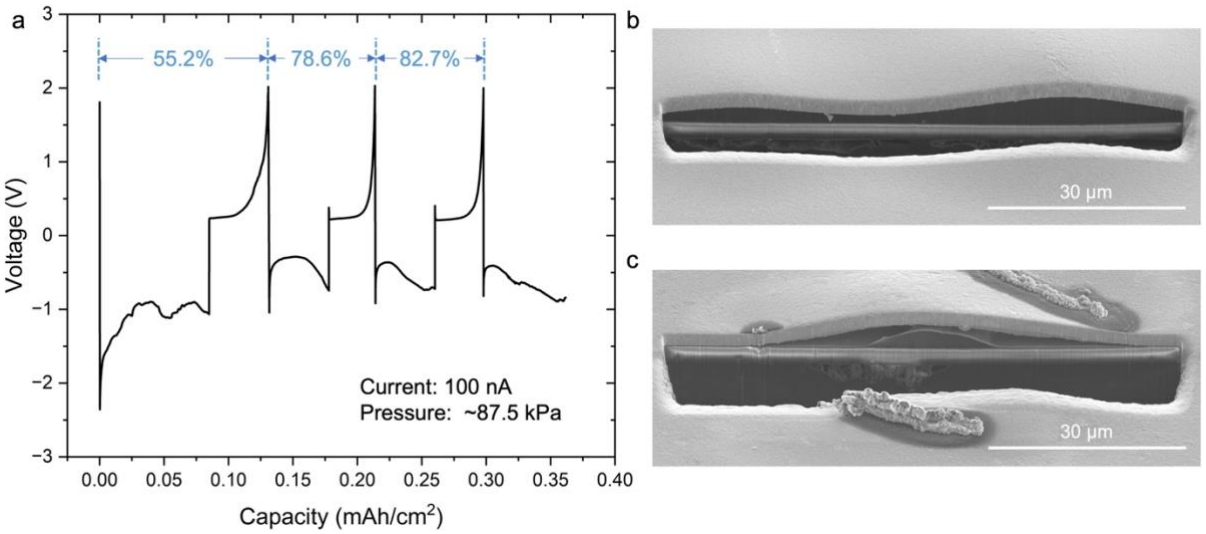


**Supplementary Fig. 12 FS-LiPON Li-Cu cell cycling with external pressure a**, Voltage curve of Li-Cu FS-LiPON cell cycled with a current of 100 nA under an external pressure of ~87.5 kPa. **b** & **c**, Cross-section images of Li-Cu cell with Au seeding layer after cycling.

As Fig. S12A shows below, a Li-Cu cell was plated with 50 μAh/cm$^2$ of Li metal in the first cycle that corresponds to a Li metal thickness of 250 nm. However, the first stripping efficiency appeared quite low as only 21%. Another cycle gave a slightly higher Coulombic efficiency of 27.1%, which is still low. The cell morphology was examined afterwards as Fig. S11B & C show. In Fig. S11B, Cu surface deforms to large bumps. Li metal cross section appeared charging under SEM, which indicates Li metal has reacted with atmosphere due to the cleavage of Cu current collector. Fig. S11C further shows a large gap generated under Cu surface after repeated Li plating/stripping, suggesting the stripping was not uniform. In order to improve the stripping uniformity, we applied external pressure of ~87.5 kPa on the cell during plating and stripping. Fig. S12A shows the voltage curve of Li-Cu FS-LiPON cell with the external pressure present. In contrast to Fig. S12A, Li-Cu cell here shows a much higher initial Coulombic efficiency of 55.2%, which ramped up to 82.7% during the third cycle. Such improvement is likely caused by the external pressure that assisted Cu to deform back when Li metal was being stripped away. We further checked the cell morphology afterwards. Fig. S12B shows the dense Li metal cross section after repeated cycling with external pressure. However, we did observe gap formation underneath Cu as Fig. S12C shows, which is in consistence with the Coulombic efficiency trend. Note that the gap was formed between Cu and FS-LiPON, which led to the disconnection of electron pathway and caused the residual inactive Li metal. This indicates that the external pressure is playing a more important role during stripping process. And by using external pressure we could largely improve the cell performance for repeatedly cycling.